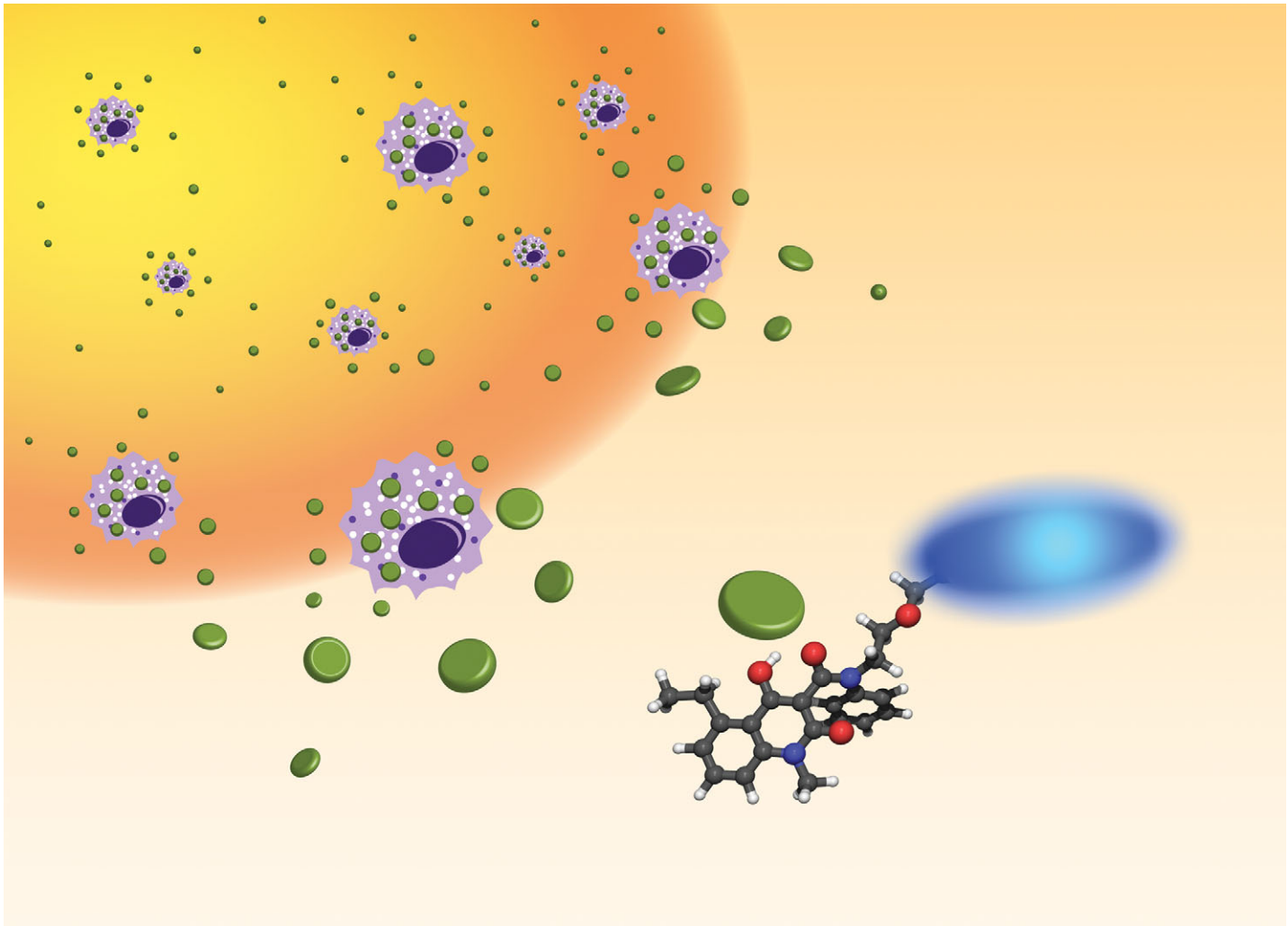

Showcasing research from the laboratory of Dr Andreas Faust, European Institute for Molecular Imaging (EIMI), University of Münster, Germany.

Development and evaluation of a non-peptidic ligand for the molecular imaging of inflammatory processes using S100A9 (MRP14) as a novel target

Here the development and first evaluation of a S100A9 specific optical imaging probe (Cy5.5-CES271) is shown. The alarmin S100A9, one subunit of the heterodimer S100A8/S100A9 (calprotectin), is locally secreted in high concentrations at sites of inflammation.

As featured in:

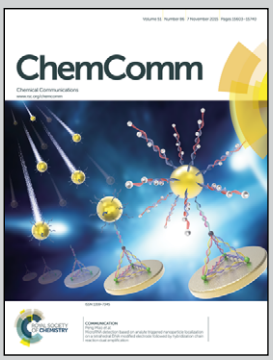

See A. Faust *et al.*, *Chem. Commun.*, 2015, **51**, 15637.

ROYAL SOCIETY OF CHEMISTRY

www.rsc.org/chemcomm

Registered charity number: 207890

ChemComm

COMMUNICATION

View Article Online
View Journal | View Issue

Cite this: *Chem. Commun.*, 2015, **51**, 15637

Received 20th August 2015,
Accepted 9th September 2015

DOI: 10.1039/c5cc07019h

www.rsc.org/chemcomm

Development and evaluation of a non-peptidic ligand for the molecular imaging of inflammatory processes using S100A9 (MRP14) as a novel target†

A. Faust,‡*[ab] T. Völler,‡[c] F. Busch,[a] M. Schäfers,[abde] J. Roth,[bce] S. Hermann[abe] and T. Vogl[bce]

The establishment of novel molecular imaging tools to monitor the local activity of inflammation remains an interdisciplinary challenge. Our target, the alarmin S100A9, one subunit of the heterodimer S100A8/S100A9 (calprotectin), is locally secreted in high concentrations from immigrated and activated phagocytes at local sites of inflammation. Calprotectin is already a well established serum biomarker for many inflammatory disorders. Here we show the development and first evaluation of the novel S100A9 specific molecular imaging probe Cy5.5-CES271 for optical imaging of local inflammatory activity *in vivo*.

Inflammatory reactions like autoimmune and infectious diseases[1] as well as cardiovascular diseases such as atherosclerosis[2] or myocardial ischemia[3] characteristically feature local immune cell activation and inflammation. These inflammatory reactions that initially serve the host by avoiding local tissue damage and by clearing infections, can in fact harm the patient during overwhelming immune responses or under chronic inflammatory conditions such as rheumatoid arthritis. The disease activity and progression, *e.g.* in atherosclerosis correlate well with the number of immigrated immune cells.[1b,4] Activated phagocytes and epithelial cells express and locally secrete high levels of the S100 protein complex S100A8/S100A9, which acts as a so called alarmin or Danger Associated Molecular Pattern (DAMP) molecule with potent pro-inflammatory capacities.[1a,4] By binding to both, the extracellular matrix and Toll-like receptor 4 (TLR4) or RAGE expressing immune cells, S100A8/S100A9 exhibits a high local concentration gradient amplifying local inflammatory reactions. Recently, S100A8/S100A9 has been established as a biomarker in many inflammatory diseases.[1a,5] S100A8/S100A9 serum levels could for example be characterized as an accurate predictor for the risk of cardiovascular events in patients. Moreover, the knockout of S100A9 significantly reduced disease severity in ApoE$^{-/-}$ mice, a mouse model for atherosclerosis.[6]

Previously, we reported the use of antibody-based optical probes such as Cy5.5™-labelled antibodies targeting the S100A9 subunit (anti-S100A9-Cy5.5) of the S100A8/S100A9 heterodimer *in vivo*. We could observe excellent correlations between signal intensity and local S100A9 expression. Furthermore, we could predict the individual disease course of a single mouse in different mouse models for inflammatory and infectious diseases.[7] However, translation of this imaging strategy into patients is challenging due to known limitations of antibody-based approaches. Therefore, we developed the first S100A9 affine optical imaging tracer based on a small non-peptidic structure, which can also be used for many other imaging modalities such as SPECT or PET when radiolabelled. We chose linomide **1** as lead compound, a synthetic immuno-modulator based on 3-quinolinecarboxamides which is firstly described in prostate 1996.[8] A modified substance of **1**, laquinimod **2** was already selected for clinical studies in man and its efficacy has been demonstrated in animal models of several autoimmune diseases, including multiple sclerosis.[9] The drug was granted a fast track review by the FDA in 2009.[10] Multivariate analytical tools were used to derive the SAR for the binding activity of a series of laquinimod analogues towards S100A9 with the assumption that similar analogs bind to the same binding site in a similar binding mode.

Recently, we could show that the most potent ligands are based on 3-quinolinecarboxamides with an ethyl group in 5-position instead of the chloride (Fig. 1).[11] We propose that the β-hydroxycarboxamide unit is responsible for binding to the protein. In comparison the quinoline moiety, where slight variations are possible, the *N*-phenyl or *N*-methylamine used for forming the

[a] *European Institute for Molecular Imaging (EIMI), University of Münster, Waldeyerstr. 15, 48149 Münster, Germany. E-mail: faustan@uni-muenster.de*
[b] *Cells-in-Motion Cluster of Excellence (EXC 1003–CiM), University of Münster, 48149 Münster, Germany*
[c] *Institute of Immunology, University Hospital of Münster, Röntgenstr. 21, 48149 Münster, Germany*
[d] *Department of Nuclear Medicine, University Hospital of Münster, Albert-Schweitzer-Campus 1, 48149 Münster, Germany*
[e] *Interdisciplinary Center for Clinical Research (IZKF Münster), University of Münster, Domagkstr. 3, 48149 Münster, Germany*

† Electronic supplementary information (ESI) available: Experimental procedures and analytical data of all compounds, details on ELISA, binding studies, mice and biodistribution. See DOI: 10.1039/c5cc07019h

‡ Authors contributed equally.

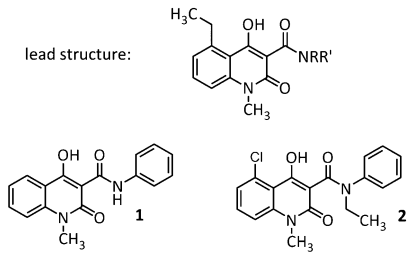

Fig. 1 Lead compound (top) and the established synthetic immunomodulators linomide **1** and laquinimod **2**.

amide bond is free for attaching different linker systems. In addition a connection of a quinolinecarboxamide on a gold surface is possible without loss of inhibition.[11]

The synthesis of the target compound **Cy5.5-CES271** for optical imaging of S100A9 is outlined in Scheme 1. Starting from the commercially available 3-nitrophthalic acid anhydride, diethyl malonate was condensed and the resulting lactone was treated with hydrochloric acid to give 2-acetyl-6-nitrobenzoic acid.[12] The anthranilic acid was synthesized in a two-step hydrogenation procedure and treated with phosgene to give the corresponding isatoic anhydride in good yield.[13] After *N*-alkylation with iodomethane the anhydride was opened with diethyl malonate under decarboxylation and reclosed yielding the corresponding β-hydroxyester. Acidic cleavage yielded the 3-quinolinecarboxylic acid **3** as key intermediate for functionalization for different labelling techniques.[14] For the first S100A9 affine imaging probe the cyanine dye Cy5.5™ label was coupled to intermediate **3** through a PEG (polyethylene glycol) linker in order to avoid interactions between the Cy5.5™ label and the protein. After the amination of the mesyl-PEG-azide[15] **4** with aniline gave low yields the mesylate was converted into the corresponding bromide and we got the secondary amine in satisfactory amounts. The key intermediate **3** was then coupled to the secondary amine and the resulting carboxamide was then reduced to give the free amine as precursor for coupling with the cyanine dye. An activated NHS-ester derivative of Cy5.5™ was added under basic conditions yielding **Cy5.5-CES271** suitable for optical imaging of S100A9.[16] For verification the HPLC-purified tracer was analyzed by high resolution mass spectrometry showing the fourfold anionic species (Scheme 1B and C).

Studies were then conducted to verify strong binding affinity of **Cy5.5-CES271** for S100A9 (Fig. 2A). In this regard, we modified our specific S100-ELISA to analyse S100A9 binding to TLR4/MD2. Instead of the capturing anti-S100A9 antibody we coated TLR4/MD2 (3146-TM-050/CF, R&D Systems) to the wells of a 96-well plate which served as capturing molecule.[7] After blocking of the unspecific binding sites by PBS/5% skim milk powder, plates were washed three times. S100A9 protein was added at a concentration of 1 μg ml^{-1} in the presence or absence of 100 μM **Cy5.5-CES271** and incubated for two hours at room temperature. Unbound S100 protein was removed by washing the plates for three times, followed by the addition of a primary anti-S100A9-antibody (1 μg ml^{-1}, polyclonal, rabbit). After a washing step, the secondary anti-rabbit-IgG-antibody coupled to HRP (1 μg ml^{-1}, Cell Signalling) was added. TMB was used as substrate for HRP to quantify binding efficiency by absorbance readings at 450 nm in an ELISA reader (Anthos Mikrosysteme). Addition of the non-peptidic S100A9 ligand (**Cy5.5-CES271**) markedly blocked binding of S100A9 to TLR4/MD2, as indicated by a decrease of signal given by the TLR4-S100A9 ELISA. These results confirm that the

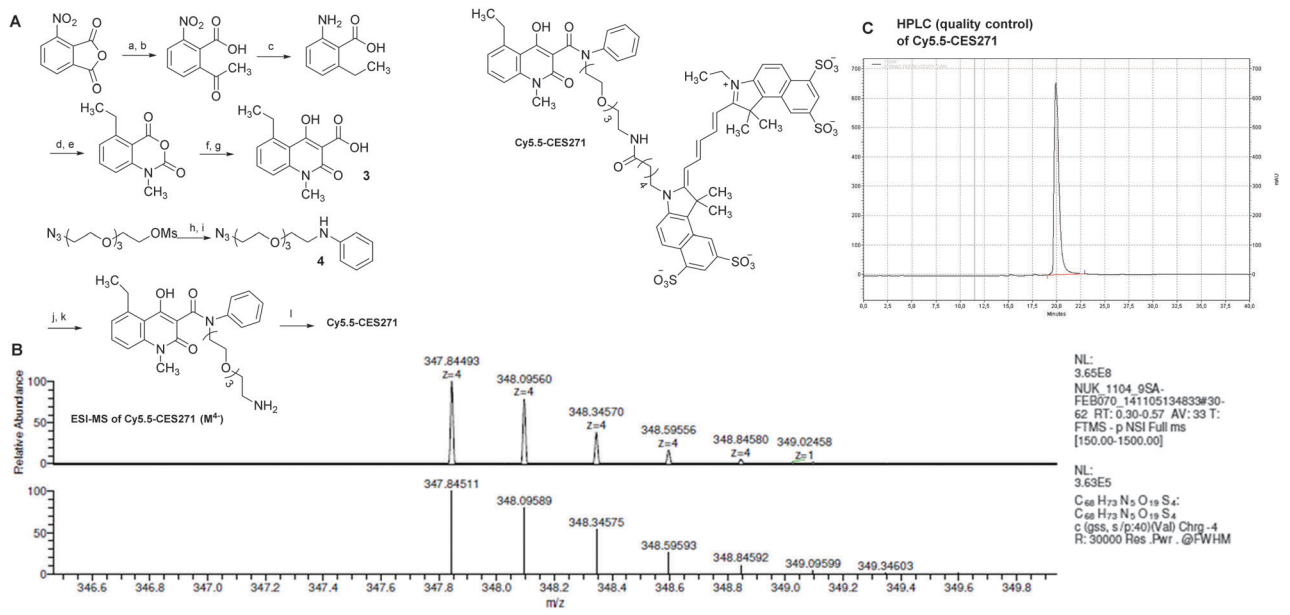

Scheme 1 (A) Synthesis of **Cy5.5-CES271**: (a) Ac_2O, NEt_3, diethyl malonate, 40 °C, 4 h, 88%; (b) HCl, H_2O, toluene, 100 °C, 14 h, 80%; (c) 1. PtO_2, H_2O, NaOH, 90 °C 3 h then rt, 14 h; 2. RANEY®-Ni, H_2O, NaOH, 110 °C, 3 h then rt, 24 h, 90% (two steps); (d) diphosgene, THF, toluene, rt, 5 h, 86%; (e) NaH, MeI, DMF, rt, 14 h; (f) NaH, diethyl malonate, DMF, 85 °C, 14 h, 53% (two steps); (g) HCl/HOAc 60 °C, 6 h, 50%; (h) LiBr, CH_3CN, reflux, 16 h, 80%; (i) aniline, H_2O, reflux, 16 h, 42%; (j) NEt_3, $SOCl_2$, CH_2Cl_2, 0 °C, 4 h, 82%; (k) H_2, Pd/C, THF, rt, 16 h, 79%; (l) Cy5.5-NHS, NEt_3, DMF, rt, 16 h, 50%. (B) Analysis and verification of **Cy5.5-CES271** (here M^{4-} species) by high resolution ESI-MS; (C) quality control (RP-HPLC) of **Cy5.5-CES271**.

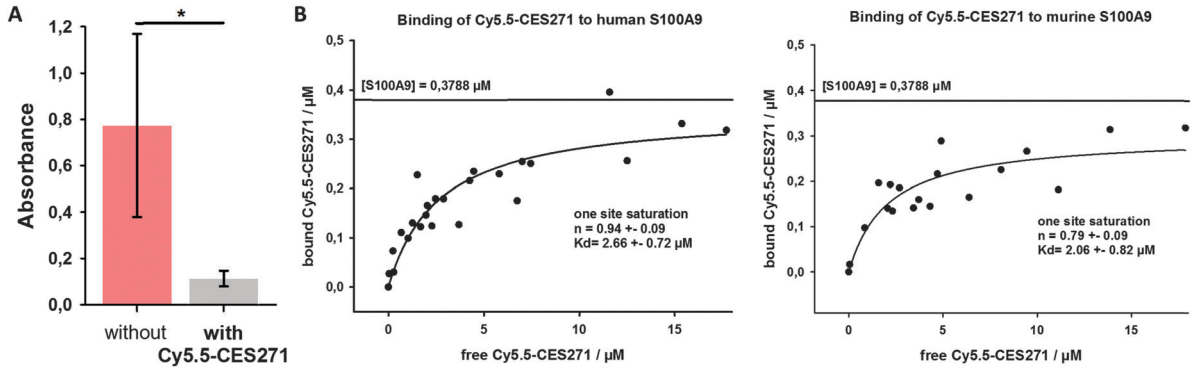

Fig. 2 (A) Analysis of the binding of **Cy5.5-CES271** to S100A9. S100A9 binding to TLR4/MD2 was quantified by an ELISA-based assay. Specific binding of **CES271-Cy5.5** to S100A9 inhibits formation of the S100A9–TLR4/MD2 complex and thereby diminishes the ELISA signal ($n = 5$; $p < 0.05$). (B) Estimation of the binding constant of **Cy5.5-CES271** to human and murine S100A9. The constant was calculated using the one site saturation regression model. Each dot represents the mean value of four independent experiments.

attachment of the dye Cy5.5 does not interfere with the binding of **Cy5.5-CES271** to S100A9. This blocking study also proves target specificity of **Cy5.5-CES271**, and shows that binding of S100A9 to TLR4/MD2 can be efficiently blocked in the presence of **Cy5.5-CES271** (resulting in low absorption).

Next, we determined the binding constants of **Cy5.5-CES271** to murine and human S100A9 by fluorimetric measurements (Fig. 2B). Briefly, 0,3788 µM S100A9 (5 µg ml^{-1} of homodimer S100A9) solved in 50 µl PBS was coated to the bottom of a 96-well plate and served as capturing molecule. For each S100A9 coated well a control well was used with 50 µl PBS alone. After a washing step, unspecific binding sites were blocked by PBS/5% skim milk powder. **Cy5.5-CES271** was added at increasing concentrations. After 1 h incubation at 4 °C, the supernatants were removed and the fluorescence intensity was measured with a fluorimeter. Non-linear regression analysis was performed with a one site saturation model, to calculate the binding constant of **Cy5.5-CES271** to either murine or human S100A9. The K_d-values of 2.66 µM (murine) and 2.06 µM (human, Fig. 2B) confirm that **Cy5.5-CES271** is eligible for imaging purposes. We observed a strong binding affinity of the tracer to S100A9 that is not affected by the attachment of Cy5.5 to CES271.

Finally, we analysed the biodistribution of **Cy5.5-CES271** injected to healthy Balb/c mice by the measurement of fluorescence intensity in various organs. Fig. 3 shows the tracer accumulation 1 and 3 h after injection. The tracer was injected at a dose of 2 nmol per mouse. We could observe a good tissue availability of **Cy5.5-CES271** and an elimination that was mainly driven by renal excretion, as indicated by the high renal uptake and the increasing concentrations of the tracer in the urinary bladder urine in comparison to the relatively low hepatic uptake. This kinetics, that is different to our previously published antibody based tracer anti-S100A9-Cy5.5[7] kinetics favors **Cy5.5-CES271** for imaging of organs neighboring the liver like the lung or the heart.

In conclusion, we developed the first optical imaging probe **Cy5.5-CES271** based on non-peptidic 3-quinolinecarboxamide for specific imaging of extracellularly released S100A9 protein indicating local phagocyte activity. The specificity was confirmed by a modified S100-ELISA and the binding potency was

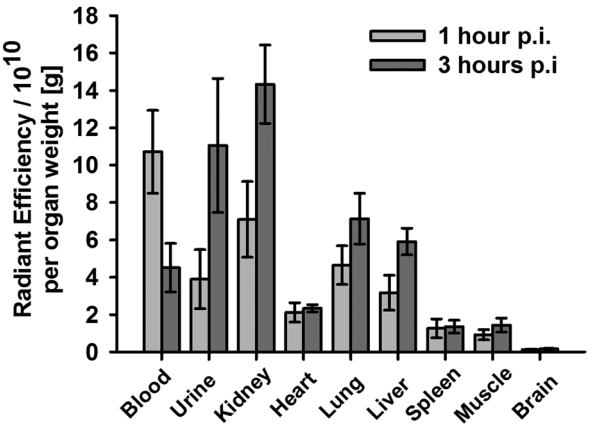

Fig. 3 Biodistribution of **Cy5.5-CES271** in healthy Balb/c mice. The tracer was intravenously injected at a dose 2 nmol per mouse. The tracer accumulation was measured 1 and 3 h post injection ($n = 5$ for each time point).

determined as sufficient for both murine and human S100A9 for *in vivo* optical imaging techniques. Ongoing *in vivo* studies in the inflamed tissue in models of ear inflammation, arthritis or myocardial infarction will give us information about the feasibility as optical probe for specific S100A9 targeted imaging. The established synthesis and imaging strategy allows further labelling methods (*e.g.* radionuclides) and is therefore suitable for clinical translation.

We gratefully acknowledge financial support from the DFG (SFB656 A9 and Z5), the Interdisciplinary Centre of Clinical Research (IZKF Münster, core unit PIX) and the Medical College Münster.

Notes and references

1 (*a*) T. Vogl, K. Tenbrock, S. Ludwig, N. Leukert, C. Ehrhardt, M. A. van Zoelen, W. Nacken, D. Foell, T. van der Poll, C. Sorg and J. Roth, *Nat. Med.*, 2007, **13**, 1042; (*b*) P. van Lent, L. C. Grevers, A. B. Blom, O. J. Arntz, F. A. van de Loo, P. van der Kraan, S. Abdollahi-Roodsaz, G. Srikrishna, H. Freeze, A. Sloetjes, W. Nacken, T. Vogl, J. Roth and W. B. van den Berg, *Arthritis Rheum.*, 2008, **58**, 3776; (*c*) P. van Lent, A. B. Blom, R. F. Schelbergen, A. Slöetjes, F. P. Lafeber, W. F. Lems, H. Cats, T. Vogl, J. Roth and W. B. van den Berg, *Arthritis Rheum.*, 2012, **64**, 1466; (*d*) K. Loser,

T. Vogl, M. Voskort, A. Lueken, V. Kupas, W. Nacken, L. Klenner, A. Kuhn, D. Foell, L. Sorokin, T. A. Luger, J. Roth and S. Beissert, *Nat. Med.*, 2010, **16**, 713; (*e*) B. Petersen, M. Wolf, J. Austermann, P. van Lent, D. Foell, M. Ahlmann, V. Kupas, K. Loser, C. Sorg, J. Roth and T. Vogl, *EMBO J.*, 2013, **9**, 100.

2 (*a*) S. Cagnin, M. Biscuola, C. Patuzzo, E. Trabetti, A. Pasquali, P. Laveder, G. Faggian, M. Iafrancesco, A. Mazzucco, P. F. Pignatti and G. Lanfranchi, *BMC Genomics*, 2009, **10**, 13; (*b*) L. A. Altwegg, M. Neidhart, M. Hersberger, S. Müller, F. R. Eberli, R. Corti, M. Roffi, G. Sütsch, S. Gay, A. von Eckardstein, M. B. Wischnewsky, T. F. Lüscher and W. Maier, *Eur. Heart J.*, 2007, **28**, 941; (*c*) K. Croce, H. Gao, Y. Wang, T. Mooroka, M. Sakuma, C. Shi, G. K. Sukhova, R. R. Packard, N. Hogg, P. Libby and D. I. Simon, *Circulation*, 2009, **120**, 427; (*d*) K. Yonekawa, M. Neidhart, L. A. Altwegg, C. A. Wyss, R. Corti, T. Vogl, M. Grigorian, S. Gay, T. F. Lüscher and W. Maie, *Atherosclerosis*, 2011, **218**, 486.

3 (*a*) J. H. Boyd, B. Kan, H. Roberts, Y. Wang and K. R. Walley, *Circ. Res.*, 2008, **102**, 1239; (*b*) D. A. Morrow, Y. Wang, K. Croce, M. Sakuma, M. S. Sabatine, H. Gao, A. D. Pradhan, A. M. Healy, J. Buros, C. H. McCabe, P. Libby, C. P. Cannon, E. Braunwald and D. I. Simon, *Am. Heart J.*, 2008, **155**, 49.

4 (*a*) J. Chan, J. Roth, J. Oppenheim, K. Tracey, T. Vogl, M. Feldmann, N. Horwood and J. Nanchahal, *J. Clin. Invest.*, 2012, **122**, 2711; (*b*) M. G. Ionita, A. Vink, I. E. Dijke, J. D. Laman, W. Peeters, P. H. van der Kraak, F. L. Moll, J. P. de Vries, G. Pasterkamp and D. P. de Kleijn, *Arterioscler., Thromb., Vasc. Biol.*, 2009, **29**, 1220.

5 D. Foell and J. Roth, *Arthritis Rheum.*, 2004, **50**, 3762.

6 M. M. Averill, C. Kerkhoff and K. E. Bornfeldt, *Arterioscler., Thromb., Vasc. Biol.*, 2012, **32**, 223.

7 T. Vogl, M. Eisenblätter, T. Völler, S. Zenker, S. Hermann, P. van Lent, A. Faust, C. Geyer, B. Petersen, K. Roebrock, M. Schäfers, C. Bremer and J. Roth, *Nat. Commun.*, 2014, **5**, 4593.

8 I. B. Joseph and J. T. Isaacs, *Prostate*, 1996, **29**, 183.

9 C. Brunmark, A. Runström, L. Ohlsson, B. Sparre, T. Brodin, M. Aström and G. Hedlund, *J. Neuroimmunol.*, 2002, **130**, 163.

10 J. Preiningerova, *Expert Opin. Invest. Drugs*, 2009, **18**, 985.

11 P. Björk, A. Björk, T. Vogl, M. Stenström, D. Liberg, A. Olsson, J. Roth, F. Ivars and T. Leanderson, *PLoS Biol.*, 2009, **7**, e1000097.

12 C. Lüthy, H. Zondler, T. Rapold, G. Seifert, B. Urwyler, T. Heinis, C. Steinrücken and J. Allen, *Pest Manage. Sci.*, 2001, **57**, 205.

13 K. Jansson, EP2316818A1, 2009.

14 S. Jönsson, G. Andersson, T. Fex, T. Fristedt, G. Hedlund, K. Jansson, L. Abramo, L. Fritzson, A. Pekarski, A. Runström, H. Sandin, I. Thuvesson and A. Björk, *J. Med. Chem.*, 2004, **47**, 2075.

15 A. Faust, B. Waschkau, J. Waldeck, C. Höltke, H. J. Breyholz, S. Wagner, K. Kopka, O. Schober, W. Heindel, M. Schäfers and C. Bremer, *Bioconjugate Chem.*, 2009, **20**, 904.

16 Labelling procedure: The amino-functionalized precursor (3.0 mg, 4.2 μmol) was dissolved in 400 μL dry dimethylformamide provided with 10 μL triethylamine. To this solution, Cy5.5-NHS ester (GE) (1 mg, 0.9 μmol) was added. The reaction mixture was vortexed for 16 h at room temperature in the dark. Purification of **Cy5.5-CES271** was performed by gradient-HPLC using a Knauer system with two K-1800 pumps, an S-2500 UV detector and a RP-HPLC Nucleosil 100–5 C_{18} column (250 mm × 4.6 mm). Eluent A: water (0.1% TFA). Eluent B: Acetonitrile (0.1% TFA). Gradient from 95% A to 40% A over 19 minutes, holding for 5 minutes and back to 95% in one minute at a flow rate of 5.5 ml min^{-1}, detection at λ = 254 nm. The appropriate fractions (t_R = 16.5 min) were collected, lyophilized, redissolved in 1 mL water and finally stored at −20 °C. The average content of **Cy5.5-CES271** was 0.45 ± 0.02 μmol ml^{-1} (≈50%) as determined by photometric measurements with λ_{abs} = 678 nm and ε_{678} = 250000 M^{-1} cm^{-1}. MS (ES^-): *m*/*z* = 464.1 (100%), 464.5, 464.8 $[M]^{3-}$; 696.7, 697.2, 697.7 $[M + H]^{2-}$. HRMS (ES^-): *m*/*z* = 347.84493, 348.09560, 348.34570, 348.59556, 348.84580 $[M]^{4-}$ calculated: 347.84511, 348.09589, 348.34575, 348.59593, 348.84592 $[M]^{4-}$.